Red, Green, and Blue Electrochromism in Ambipolar Poly(amine–amide–imide)s Based on Electroactive Tetraphenyl-*p*-Phenylenediamine Units

LI-TING HUANG, HUNG-JU YEN, CHA-WEN CHANG,* GUEY-SHENG LIOU

Functional Polymeric Materials Laboratory, Institute of Polymer Science and Engineering, National Taiwan University, 1 Roosevelt Road, 4th Section, Taipei 10617, Taiwan

Received 25 June 2010; accepted 29 July 2010
DOI: 10.1002/pola.24266
Published online 20 September 2010 in Wiley Online Library (wileyonlinelibrary.com).

ABSTRACT: A series of novel poly(amine–amide–imide)s (PAAIs) based on tetraphenyl-*p*-phenylenediamine (TPPA) units showing anodically/cathodically electrochromic characteristic with three primary colors [red, green, and blue (RGB)] were prepared from the direct polycondensation of the TPPA-based diamine monomer with various aromatic bis(trimellitimide)s. These multicolored electrochromic polymers were readily soluble in polar organic solvents and showed excellent thermal stability associated with high glass-transition temperatures (288–314 °C) and high-char yield (higher than 60% at 800 °C in nitrogen). The PAAI films revealed electrochemical oxidation and reduction accompanied with high contrast of optical transmittance color changes from the pale yellow neutral state to the green/blue oxidized state and red reduced state, respectively. The electrochromic films had high-coloration efficiency (CE = 178 and 242 cm^2/C at the first and the second stages, respectively), low-switching time, and good redox stability, which still retained a high electroactivity after long-term redox cycles. © 2010 Wiley Periodicals, Inc. J Polym Sci Part A: Polym Chem 48: 4747–4757, 2010

KEYWORDS: electrochemistry; electrochromism; functionalization of polymers; polyimides; triphenylamine

INTRODUCTION Electrochromic materials show a reversible optical change ability in absorption or transmittance upon electrochemically oxidized or reduced, which has stimulated the interest of scientists over the past decades.[1] Early, investigation of electrochromic materials has been interested in optical properties in the visible region change (400–800 nm), proved useful and variable applications such as e-paper, optical switching devices, smart window, and camouflage materials.[2] There are many intrinsically electrochromic materials, such as transition-metal oxides, inorganic coordination complexes, organic molecules, and conjugated polymers.[3] Increasingly, attention of the optical changes has been focused extending from the near infrared (NIR; e.g., 800–2000 nm) through the microwave regions of the spectrum, which could be exploitable for optical communication, data storage, and environmental control (heat gain or loss) in buildings.[4] Therefore, NIR electrochromic materials including transition metal oxides (WO3), organic metal complex (ruthenium dendrimer), and quinone-containing organic materials have been investigated in recent years.[5] For organic materials, *N,N,N′,N′*-tetraphenyl-*p*-phenylenediamine (TPPA)-containing molecule is a interesting anodic electrochromic system for NIR applications due to its particular intramolecular electron transfer (ET) in the oxidized states.

Intramolecular ET processes were studied extensively in the mixed-valence (MV) systems[6] and usually used one-dimensional MV compounds contain two or more redox states connected via σ- or π-bridge molecule. According to Robin and Day,[7] the TPPA cation radical has been reported as a symmetrical delocalized Class III structure with a strong electronic coupling (the electron is delocalized over the two redox centers), leading an intervalence charge transfer (IV-CT) absorption band in the NIR region.[8]

Triarylamine derivatives are well known as its photo- and electro-active properties that have potentials for optoelectronic applications, such as photoconductors, hole-transporters, light-emitters, and memory devices.[9] Electron-rich triarylamines can be easily oxidized to form stable radical cations, and the oxidation process is always associated with a noticeable change of coloration. Thus, investigations of the synthesis and electrochromism of triarylamine-based polymers have been reported in the literature.[10] In 2005, our groups have initiated several high-performance polymers (e.g., aromatic polyamides and polyimides) utilizing the triarylamine unit as an electrochromic functional moiety.[11] In our continuous effort to develop triphenylamine (TPA)-based electrochromic high-performance polymers,[12] they showed good electrochromic reversibility in the visible and NIR regions. However, most of the polymers studied so far mainly reveal green and blue electrochromic behaviors. According to the previous reports, polyimides can undergo reversible electrochemical reduction reactions with strong absorbances in the visible spectral region at the stable reduced (radical-anion and -dianion) forms.[13] The electroactive centers have been identified as the aromatic-carbonyl π-system of the imide functional

**Present address:* Department of Organic and Polymeric Materials, Tokyo Institute of Technology, Meguro-Ku, Tokyo, Japan.
Additional Supporting Information may be found in the online version of this article. Correspondence to: G.-S. Liou (E-mail: gsliou@ntu.edu.tw)
Journal of Polymer Science: Part A: Polymer Chemistry, Vol. 48, 4747–4757 (2010)

groups. Hence, our strategy was to synthesize the highly stable NIR electroactive TPPA-based materials with the incorporation of strong electron-withdrawing phthalimide groups, thus could afford desirable characteristics such as excellent thermal stability, good physical properties, and the interesting electrochemical and multielectrochromic behaviors. The electroactive polymers could be obtained readily by using conventional polycondensation methods and exhibited high molecular weights. Because of the incorporation of packing-disruptive TPPA units into the polymer backbone, most of the polymers exhibited good solubility in polar organic solvents, thus transparent and flexible polymer thin films could be easily prepared by solution casting and spin-coating techniques. This is useful for their fabrication of large area, thin-film electrochromic devices.

In this article, we therefore used the diamine monomer, *N,N*-bis(4-aminophenyl)-*N′,N′*-di(4-methoxyphenyl)-1,4-phenylenediamine [$(OMe)_2$TPPA-diamine; **I**] to prepare a series of aromatic poly(amine–amide–imide)s (PAAIs) containing electroactive TPPA units with para-substituted methoxy groups. The incorporation of electron-donating substituents is expected to reduce the oxidation potential associated with increased electrochemical and electrochromic stability of the resulted polymers.[14] Replacement of polyimides by copolyimides such as PAAIs may be useful in modifying the intractable character of polyimides. Because of the combination of both amide and imide groups in polymer repeating units, PAAIs have structural and physical similarity between polyamides and polyimides; correspondingly, these polymers offer a good compromise between high-thermal property and processability. Thus, we anticipated that the prepared electroactive PAAIs would reveal multielectrochrmic behaviors, high-electrochemical stability, improved optical response times, and enhanced contrast of optical transmittance in NIR region. For a comparative study, some properties of the present PAAIs will be compared with those of structurally related one based on *N,N′*-bis(4-aminophenyl)-*N,N′*-diphenyl-1,4-phenylenediamine [TPPA-diamine; **I′**] that has been reported previously.[11(a)]

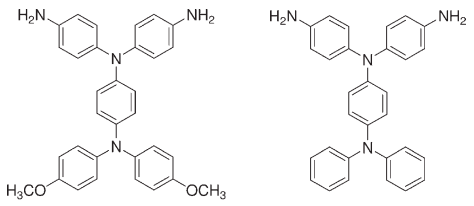

I **I′**

EXPERIMENTAL

Materials

A $(OMe)_2$TPPA-containing aromatic diamine, *N,N*-bis(4-aminophenyl)-*N′,N′*-di(4-methoxyphenyl)-1,4-phenylenediamine (**I**), was synthesized by the cesium fluoride-mediated condensation of 4-amino-4′,4″-dimethoxytriphenylamine with 4-fluoronitrobenzene, followed by palladium-catalyzed hydrazine reduction of the dinitro intermediate according to a previously reported procedure.[14(b)] 2,5-Bis(trimellitimido)toluene[15] (**II-M**), 1,4-bis (trimellitimido)-2,5-dimethylbenzene[16] (**II-2M**), and 1,4-bis(trimellitimido)-2,5-dichlorobenzene[17] (**II-2Cl**) were prepared as previously reported procedures. Tetrabutylammonium perchlorate (TBAP) (ACROS) was recrystallized twice from ethyl acetate and then dried *in vacuo* before use. All other reagents were used as received from commercial sources.

Polymer Synthesis

The synthesis of poly(amine–amide–imide) **PAAI-2M** was used as an example to illustrate the general synthetic route used to produce the PAAIs. A mixture of 0.5026 g (1.00 mmol) of the diamine monomer **I**, 0.4703 g (1.00 mmol) of 1,4-bis(trimellitimido)-2,5-dimethylbenzene (**II-2M**), 0.12 g of calcium chloride, 1.00 mL of triphenyl phosphite (TPP), 0.50 mL of pyridine, and 1.00 mL of *N*-methyl-2-pyrrolidinone (NMP) was heated with stirring at 105 °C for 3 h. The obtained polymer solution was poured slowly into 300 mL of stirred methanol giving rise to a stringy, fiber-like precipitate that was collected by filtration, washed thoroughly with hot water and methanol, and dried under vacuum at 100 °C. Reprecipitations of the polymer by *N,N*-dimethylacetamide (DMAc)/methanol were carried out twice for further purification. The inherent viscosity and weight-average molecular weights (M_w) of the obtained polymer **PAAI-2M** were 0.53 dL/g (measured at a concentration of 0.5 g/dL in DMAc at 30 °C) and 93,500 Da, respectively. The Fourier transform infrared (FTIR) spectrum of **PAAI-2M** (film) exhibited characteristic amide absorption bands at 3372 cm^{-1} (N—H stretch), 1660 cm^{-1} (amide carbonyl), imide absorption bands at 1778 cm^{-1} (asymmetrical C=O), 1724 cm^{-1} (symmetrical C=O), 1357 cm^{-1} (C—N), and 725 cm^{-1} (imide ring deformation).

^{1}H NMR (DMSO-d_6, δ, ppm): 2.17 (s, 6H, CH_3), 3.73 (s, 6H, OCH_3), 6.80 (d, 2H, H_c), 6.90 (d, 4H, H_f), 6.93 (d, 2H, H_d), 7.01 (d, 4H, H_e), 7.03 (d, 4H, H_b), 7.49 (s, 2H, H_j), 7.75 (d, 4H, H_a), 8.16 (d, 2H, H_h), 8.47 (d, 2H, H_g), 8.58 (s, 2H, H_i), 10.60 (s, 2H, NH—CO). ^{13}C NMR (DMSO-d_6, δ, ppm): 17.0 (CH_3), 55.1 (OCH_3), 114.8, 121.5, 121.7, 122.2, 123.0, 123.8, 125.2, 125.7, 125.9, 131.1, 131.4, 131.8, 133.3, 133.7, 134.3, 134.8, 140.1, 140.4, 143.7, 143.9, 155.3, 163.1 (NH—CO), 166.2, 166.4. Anal. Calcd. for $C_{58}H_{42}N_6O_8$ (950.99): C, 73.25%; H, 4.45%; N, 8.84%. Found: C, 68.07%; H, 5.48%; N, 8.27%.

The fourier transform infrared (FT-IR) and ^{1}H NMR spectra of **PAAI-2M** are shown in Supporting Information (see Figs. S1 and S2). The other PAAIs were prepared by an analogous procedure (see Supporting Information Fig. S1).

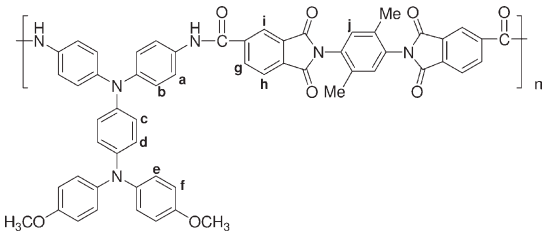

Preparation of the Poly(amine–amide–imide) Films

A solution of polymer was made by dissolving about 0.7 g of the PAAI sample in 10 mL of DMAc. The homogeneous solution was poured into a 9-cm glass Petri dish, which was placed in a 90 °C oven for 2 h to remove most of the solvent; then the semidried film was further dried *in vacuo* at

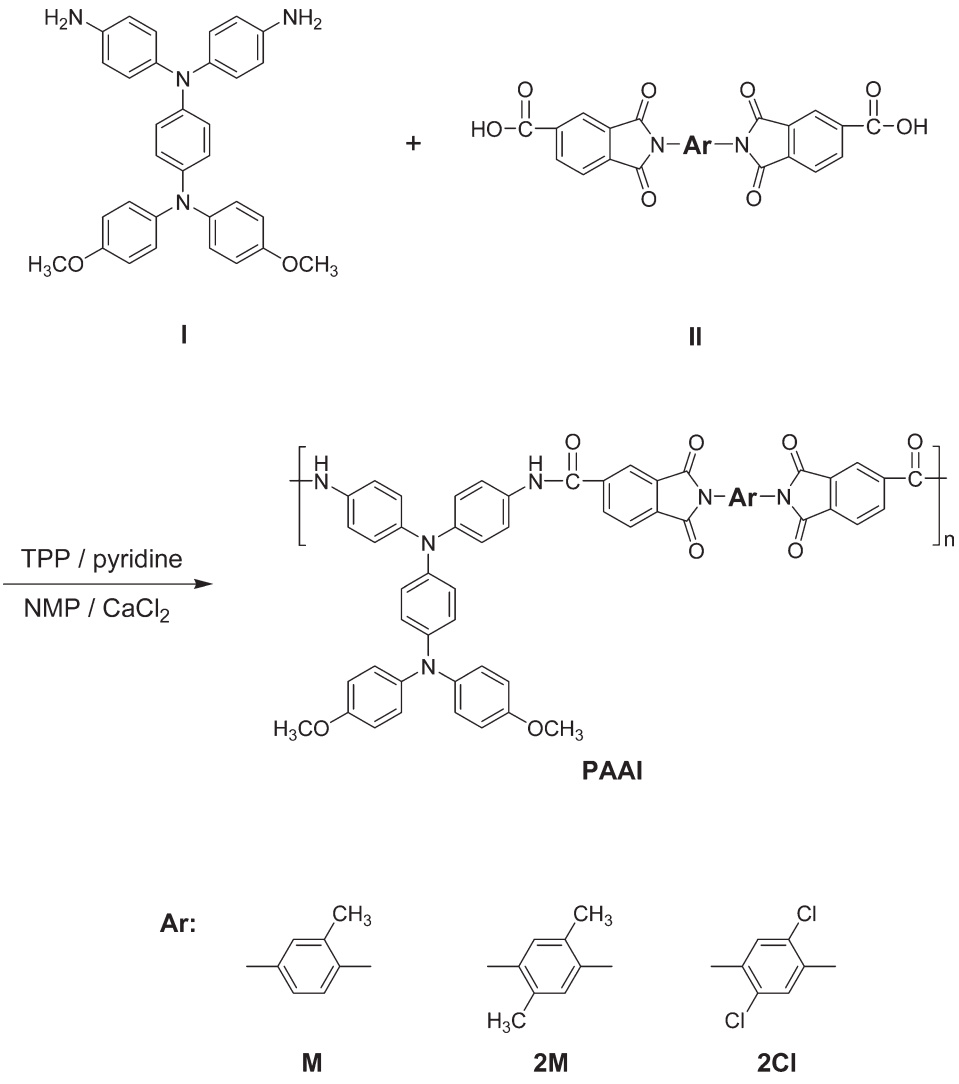

SCHEME 1 Synthesis of poly (amine–amide–imide)s.

160 °C for 8 h. The obtained films were about 50–75 μm in thickness and were used for solubility tests and thermal analyses.

Measurements

FTIR spectra were recorded on a PerkinElmer Spectrum 100 Model FTIR spectrometer. ^{1}H and ^{13}C NMR spectra were measured on a Bruker AC-300 MHz spectrometer in deuterated dimethyl sulfoxide (DMSO-d_6), using tetramethylsilane as an internal reference, and peak multiplicity was reported as follows: s, singlet; d, doublet. Elemental analyses were run in a Heraeus VarioEL-III CHNS elemental analyzer. The inherent viscosities were determined at 0.5 g/dL concentration using Tamson TV-2000 viscometer at 30 °C. Gel permeation chromatographic analysis was carried out on a Waters chromatography unit interfaced with a Waters 2410 refractive index detector. Two Waters 5 μm Styragel HR-2 and HR-4 columns (7.8 mm I.D. × 300 mm) were connected in series with NMP as the eluent at a flow rate of 0.5 mL/min at 60 °C and were calibrated with polystyrene standards. Thermogravimetric analysis (TGA) was conducted with a Perkin Elmer Pyris 1 TGA. Experiments were carried out on ~6–8 mg film samples heated in flowing nitrogen or air (flow rate = 20 cm^3/min) at a heating rate of 20 °C/min. Differential scanning calorimetry (DSC) analyses were performed on a PerkinElmer Pyris 1 DSC at a scan rate of 20 °C/min in flowing nitrogen (20 cm^3/min). Electrochemistry was performed with a CH Instruments 611B electrochemical analyzer. Voltammograms are presented with the positive potential pointing to the left and with increasing anodic currents pointing downward. Cyclic voltammetry (CV) was conducted with the use of a three-electrode cell in which indium tin oxide (ITO) (polymer films area about 0.5 cm × 1.1 cm) was used as a working electrode. A platinum wire was used as an auxiliary electrode. All cell potentials were taken by using a homemade Ag/AgCl, KCl (sat.) reference electrode. Ferrocene was used as an external reference for calibration [0.44 V vs. Ag/AgCl in CH_3CN; 0.52 V vs. Ag/AgCl in dimethylformamide (DMF)]. Spectroelectrochemical experiments were carried out in a cell built from a 1 cm commercial ultraviolet (UV)–visible cuvette using Hewlett-Packard 8453 UV–Visible diode array UV–vis–NIR spectrophotometer. The ITO-coated glass

TABLE 1 Thermal Properties of Poly(amine–amide–imide)s

Polymer Code	T_g (°C)[a]	T_d at 5% Weight Loss (°C)[b]		T_d at 10% Weight Loss (°C)[b]		Char Yield (wt %)[c]
		N_2	Air	N_2	Air	
PAAI-M	288	490	485	520	535	60
PAAI-2M	314	485	480	520	530	63
PAAI-2Cl	302	475	480	510	515	62

[a] Midpoint temperature of baseline shift on second DSC heating trace (rate 20 °C/min) of the sample after quenching from 400 °C.
[b] Decomposition temperature, recorded via TGA at a heating rate of 20 °C/min and a gas-flow rate of 20 cm^3/min.
[c] Residual weight percentage at 800 °C in nitrogen.

slide was used as the working electrode, a platinum wire as the counter electrode, and an Ag/AgCl cell as the reference electrode. Coloration efficiency (CE) (η) determines the amount of optical density change (δOD) at a specific absorption wavelength induced as a function of the injected/ejected charge (Q; also termed as electroactivity), which is determined from the *in situ* experiments. CE is given by the equation: $\eta = \delta OD/Q = \log[T_b/T_c]/Q$, where η (cm^2/C) is the CE at a given wavelength, and T_b and T_c are the bleached and colored transmittance values, respectively. The thickness of the PAAI thin films was measured by alpha-step profilometer (Kosaka Lab., Surfcorder ET3000, Japan).

RESULTS AND DISCUSSION

Polymer Synthesis

According to the phosphorylation polyamidation technique described by Yamazaki,[18] a series of novel $(OMe)_2$TPPA-based PAAIs were synthesized from the polycondensation reactions of diamine monomer **I** with three aromatic diimide–diacids **II** by using TPP and pyridine as condensing agents (Scheme 1). All polymerization reactions proceeded homogenously and gave high-viscous polymer solution, which precipitated in a tough, fiber-like form when the resulting polymer solutions were slowly poured into stirring methanol. The obtained PAAIs had inherent viscosities in the range of 0.28–0.61 dL/g with weight-average molecular weights (M_w) and polydispersity of 84,900–103,100 Da and 1.75–2.18, respectively, relative to polystyrene standards as summarized in Supporting Information Tables S1 and S2. All the polymers can be solution-cast into flexible and transparent films, indicating the formation of high molecular weight polymers. The structures of the PAAIs were confirmed by IR spectroscopy. As shown in Supporting Information Figure S1, a typical IR spectrum for **PAAI-2M** exhibited characteristic absorption bands of the amide group at around 3372 cm^{-1} (N—H stretch) and 1660 cm^{-1} (amide carbonyl), and the characteristic imide absorption bands at 1778 (asymmetrical C=O), 1724 (symmetrical C=O), 1357 (C—N), and 725 cm^{-1} (imide ring deformation). Supporting Information Figure S2 shows a typical ^{1}H NMR spectrum of **PAAI-2M** in DMSO-d_6, where all peaks have been assigned to the hydrogen atoms, and the spectra agree well with the proposed molecular structure of **PAAI-2M**. A structurally related **PAAI-2M′** derived from diamine **I′** is used for comparison studies. The synthesis and characterization of polymer **PAAI-2M′** has been described previously.[19]

Solubility and Film Property

The solubility properties of polymers were investigated qualitatively, and the results are also listed in Supporting Information Table S1. Most of the PAAIs were readily soluble in polar aprotic organic solvents such as NMP, DMAc, and dimethyl sulfoxide (DMSO) at room temperature and formed flexible, tough, and transparent films by solution casting. Their high solubility and amorphous properties can be attributed to the incorporation of bulky, three-dimensional $(OMe)_2$TPPA moiety along the polymer backbone, which results in a high steric hindrance for close packing, and thus reduces their crystallization tendency. Therefore, the excellent solubility makes these polymers as potential candidates for practical applications by spin-coating or inkjet-printing processes to afford high-performance thin films for optoelectronic devices.

Thermal Properties

The thermal properties of PAAIs were investigated by TGA and DSC, and the thermal behavior data are summarized in Table 1. Typical TGA curves of representative polymer **PAAI-**

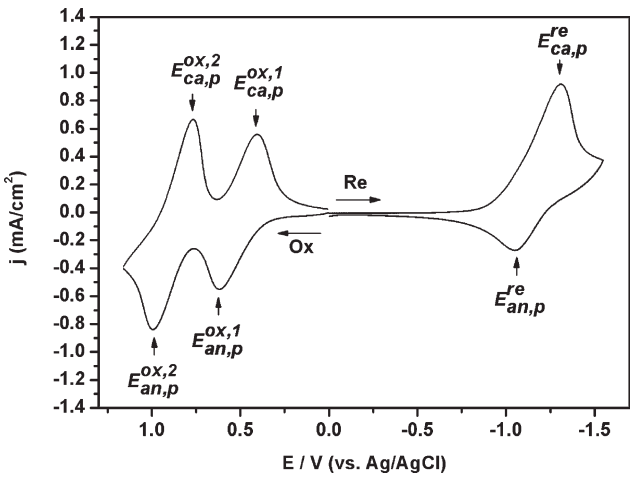

FIGURE 1 Cyclic voltammetric diagram of **PAAI-2M** film on ITO-coated glass substrate in CH_3CN (oxidation) and DMF (reduction) solutions containing 0.1 M TBAP at scan rate of 50 and 100 mV/s, respectively.

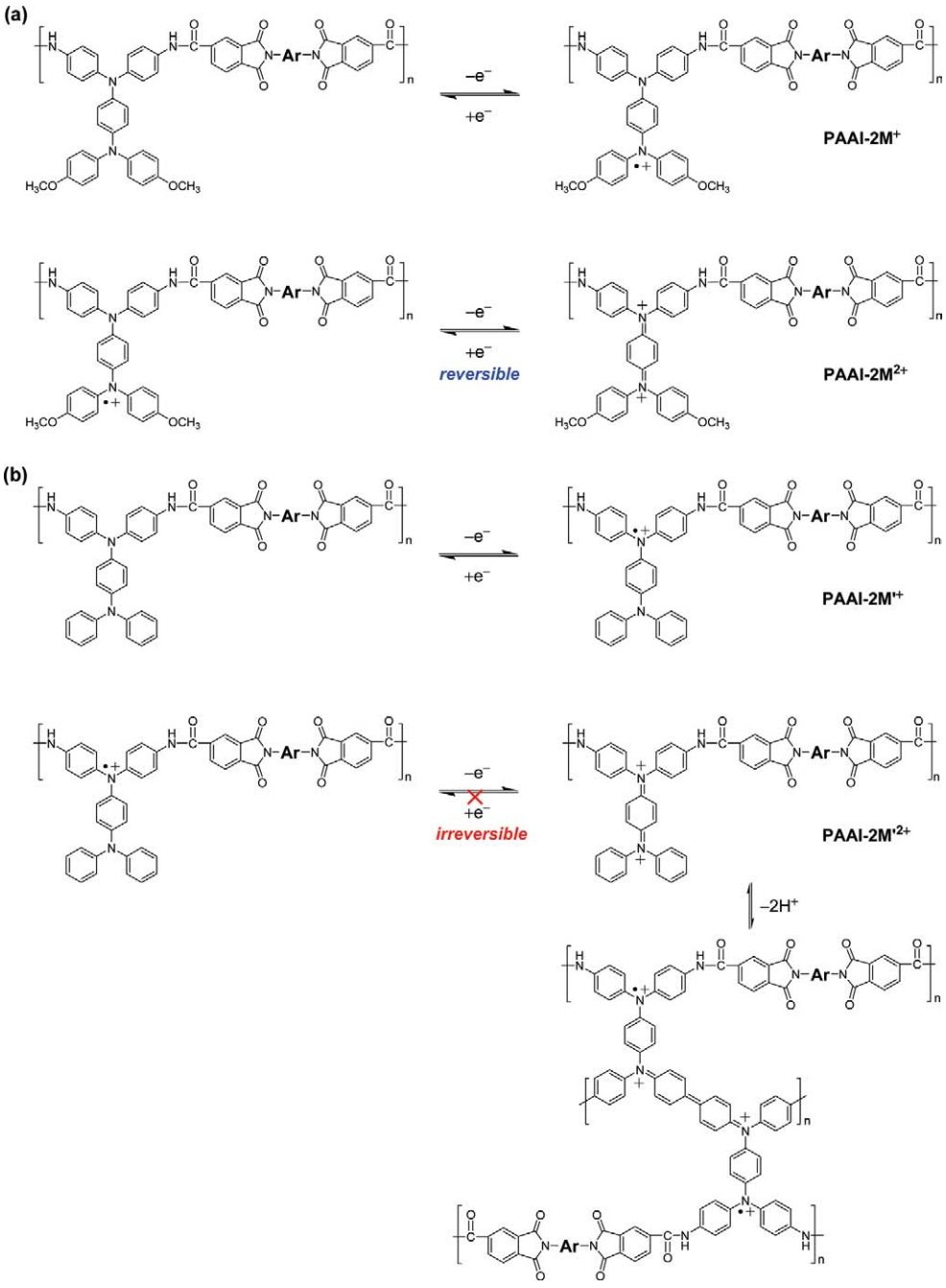

SCHEME 2 The anodic oxidation pathways of poly(amine–amide–imide)s **PAAI-2M** and **PAAI-2M′**. [Color figure can be viewed in the online issue, which is available at wileyonlinelibrary.com.]

2M in both air and nitrogen atmospheres are shown in Supporting Information Figure S3. All the prepared PAAIs exhibited good thermal stability with insignificant weight loss up to 400 °C in nitrogen. The 10% weight loss temperatures of these polymers in nitrogen and air were recorded in the range of 510–520 °C and 515–535 °C, respectively. The amount of carbonized residue (char yield) of these polymers in a nitrogen atmosphere was more than 60% at 800 °C. The high-char yields of these polymers can be ascribed to their high-aromatic content. The glass-transition temperatures (T_g) of PAAIs could be easily measured in the DSC thermograms; they were observed in the range of 288–314 °C (as shown in Supporting Information Fig. S4). The lowest T_g value of **PAAI-M** in this series polymers can be explained in terms of less steric hindrance in its diimide–diacid component. All the polymers indicated no clear melting endotherms up to the decomposition temperatures on the DSC thermograms, which supports the amorphous nature of these PAAIs.

Electrochemical Properties

The electrochemical properties of the PAAIs were investigated by CV conducted for the cast film on an ITO-coated glass substrate as working electrode. The oxidation and reduction cycles of the film samples were measured in acetonitrile (CH_3CN) and DMF, respectively, using 0.1 M of TBAP as a supporting electrolyte under a nitrogen atmosphere for

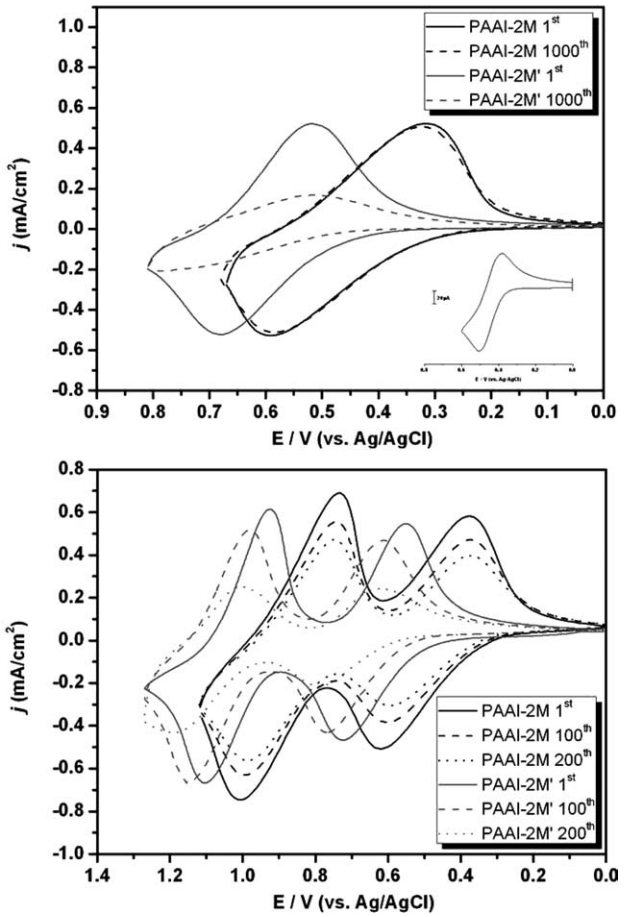

FIGURE 2 Cyclic voltammetric diagrams of poly(amine–amide–imide) **PAAI-2M** and **PAAI-2M′** films on an ITO-coated glass substrate over cyclic scans and ferrocene (inset) in 0.1 M TBAP/CH_3CN at a scan rate of 50 mV/s.

oxidation and reduction measurements. Typical CV curves of **PAAI-2M** are shown in Figure 1. All the PAAIs exhibited two reversible oxidation and one reduction processes (see Supporting Information Fig. S5), revealing their high-electrochemical stability for both *p*- and *n*-doping (ambipolar) process, and these results are similar to the previous reports of ambipolar polymers.[20] These reversible oxidation redox waves represent the formation of stable radical cation and radical dication originating from electrochemical redox reactions of the $(OMe)_2$TPPA [Scheme 2(a)]. To understand the reduction redox properties of PAAIs, we choose the simplest structure of polyimide, Kapton® to undergo electrochemical reduction. The representative cyclic voltammogram for Kapton® is shown in Supporting Information Figure S6. The pyromellitimide segment undergoes two reversible ETs with the first reduced step at the half-wave potential ($E_{1/2}$) of −0.83 V corresponding to reduction of the neutral form to the radical anion, and the second reduced couple at −1.34 V relates to further reduction of the radical anion to the dianion state.[13] The redox mechanism associated with the reduction of Kapton® has been proposed (Supporting Information Scheme S1).[13(a)] The observed electrochemical reduction of the PAAIs are similar to the previous report,[21] confirming the imide's carbonyl group as the electroactive site.

The typical CV for polymer **PAAI-2M** (with 4,4′-dimethoxy-substituted) and **PAAI-2M′** (without 4,4′-dimethoxy-substituted) is shown in Figure 2 for comparison; there are two reversible oxidation redox couples at the half-wave potential ($E_{1/2}$) of 0.51 V (E_{onset} = 0.36) and 0.87 V for **PAAI-2M**, 0.64 (E_{onset} = 0.51) and 1.01 V for **PAAI-2M′** in the oxidative scan, respectively. When comparing the electrochemical data, it was found that **PAAI-2M** is more easily oxidized than **PAAI-2M′**. Obviously, the lower oxidation potential of **PAAI-2M** compared with its analog **PAAI-2M′** can be attributed to the para-position substituted electron-donating methoxy group on TPPA groups. During the electrochemical oxidation of the PAAI thin films, the color of the film changed from pale yellow to green and then to blue. Because of the high-electrochemistry stability, **PAAI-2M** exhibited reversible CV behavior by continuous 1000 cyclic and 200 cyclic scans in the first- and second-oxidation stages, respectively. On the contrary, the corresponding **PAAI-2M′** without the para-methoxy substituted on TPPA units gradually lost redox reversibility after several CV scans. This result also confirms that para-substitution of the methoxy group on the TPPA unit effectively increases stability for both the cation radical and dication quinonediimine species. According to these results, mechanisms of oxidation reactions for **PAAI-2M** and **PAAI-2M′** are proposed in Scheme 2. The redox potentials of the PAAIs and their respective highest occupied molecular orbital and lowest unoccupied molecular orbital (vs. vacuum) are shown in Table 2.

TABLE 2 Redox Potentials and Energy Levels of Poly(amine–amide–imide)s

	Thin Films	Oxidation[a]			Reduction[b]			Oxidation		Reduction		
Polymer	λ_{onset}	E_{onset}	$E_{1/2(ox1)}$	$E_{1/2(ox2)}$	E_{onset}	$E_{1/2}$	E_g^{Opt} (eV)	HOMO[c]	LUMO[d]	HOMO[e]	LUMO[f]	E_g^{EC} (eV)
PAAI-M	571	0.39	0.52	0.89	−0.85	−1.15	2.17	4.88	2.71	5.30	3.13	1.93
PAAI-2M	583	0.36	0.51	0.87	−0.87	−1.18	2.12	4.87	2.75	5.22	3.10	1.92
PAAI-2Cl	566	0.42	0.54	0.90	−0.81	−1.13	2.19	4.90	2.71	5.34	3.15	1.93

[a] From cyclic votammograms versus Ag/AgCl in CH_3CN. $E_{1/2}$: Average potential of the redox couple peaks.
[b] From cyclic votammograms versus Ag/AgCl in DMF. E_g^{Opt}, optical band gap is derived from polymer films ($E_g^{Opt} = 1240/\lambda_{onset}$); E_g^{EC}, electrochemical band gap is derived from the difference between the $E_{an,p}^{ox,1}$ and $E_{ca,p}^{re}$.
[c] The HOMO energy levels were calculated from cyclic voltammetry and were referenced to ferrocene ($E_{1/2}$ = 0.44 V).
[d] LUMO = HOMO − E_g^{Opt}.
[e] HOMO = LUMO + E_g^{Opt}.
[f] The LUMO energy levels were calculated from cyclic voltammetry and were referenced to ferrocene ($E_{1/2}$ = 0.52 V).

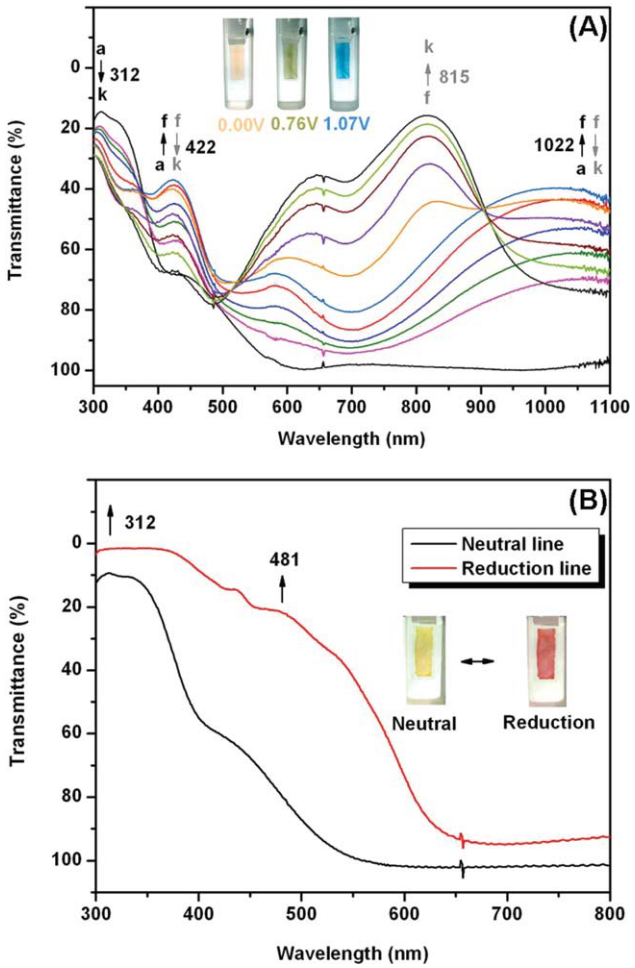

FIGURE 3 Electrochromic behavior of poly(amine–amide–imide) PAAI-2M film on the ITO-coated glass substrate in (A) 0.1 M TBAP/CH_3CN at applied potentials of (a) 0.00, (b) 0.52, (c) 0.55, (d) 0.58, (e) 0.64, (f) 0.76, (g) 0.87, (h) 0.90, (i) 0.93, (j) 0.96, and (k) 1.07 V (vs. Ag/AgCl), PAAI-2M$^+$, black solid arrow; PAAI-2M^{2+}, gray solid arrow and (B) 0.1 M TBAP/DMF at applied potentials from 0 to −2.00 V (vs. Ag/AgCl).

Spectroelectrochemistry

Spectroelectrochemical experiments were used to evaluate the optical properties of the electrochromic films. For the investigations, the PAAI film was cast on an ITO-coated glass slide (a piece that fit in the commercial UV–visible cuvette), and a homemade electrochemical cell was built from a commercial ultraviolet (UV)-visible cuvette. The cell was placed in the optical path of the sample light beam in a UV–vis-NIR spectrophotometer, which allowed us to acquire electronic absorption spectra under potential control in a 0.1 M TBAP/CH_3CN solution for oxidation and 0.1 M TBAP/DMF solution for reduction, respectively. The result of the **PAAI-2M** film upon oxidation and reduction are presented in Figure 3 as a series of UV–vis-NIR absorbance curves correlated to electrode potentials. Figure 4 shows the three-dimensional % transmittance wavelength–applied potential correlations of this sample. The **PAAI-2M** film exhibited strong absorption

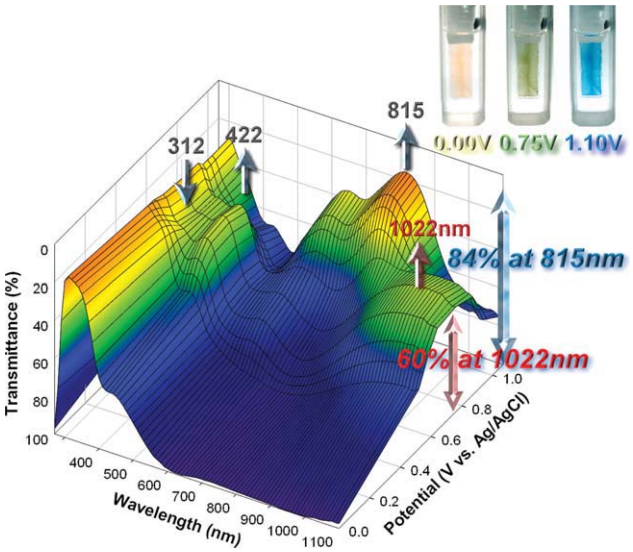

FIGURE 4 Three-dimensional spectroelectrochemical behavior of **PAAI-2M** thin film on the ITO-coated glass substrate in 0.1 M TBAP/CH_3CN from 0 to 1.07 V (vs. Ag/AgCl).

at around 312 nm, characteristic for triarylamine unit in the neutral form (0 V), with almost transparent at wavelengths >600 nm. Upon oxidation (increasing applied voltage from 0 to 0.76 V), the intensity of the absorption peak at 312 nm gradually decreased, whereas a new peak at 422 nm and a

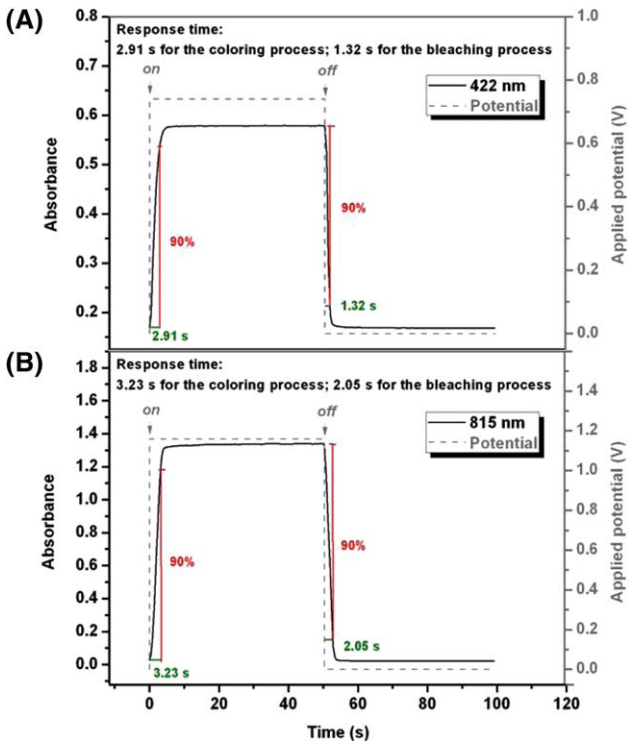

FIGURE 5 Calculation of optical switching time at (A) 422 nm and (B) 815 nm at the applied potential curves of **PAAI-2M** thin film (~300 nm in thickness) on the ITO-coated glass substrate (coated area: 1.1 cm × 0.5 cm) in 0.1 M TBAP/CH_3CN.

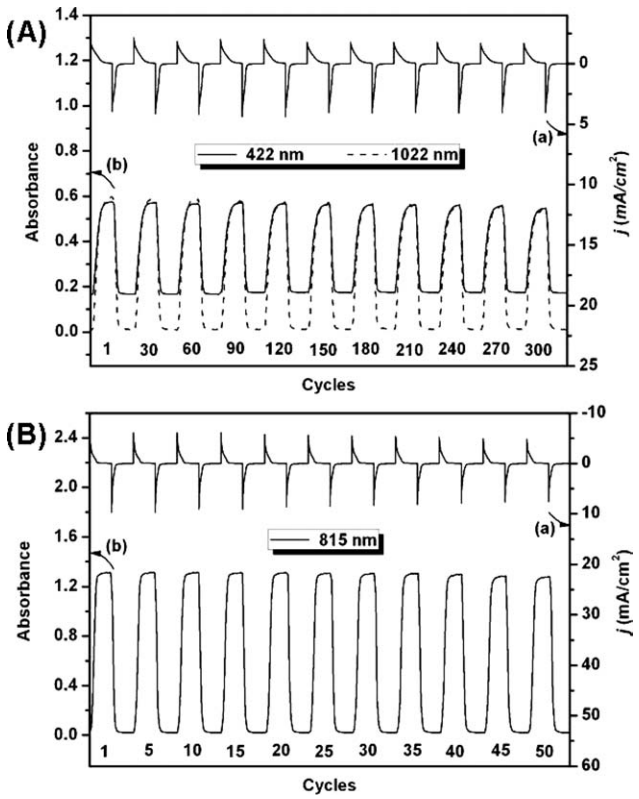

FIGURE 6 Electrochromic switching between (A) 0 and 0.74 V and (B) 0 and 1.16 V (vs. Ag/AgCl) of **PAAI-2M** thin film (~300 nm in thickness) on the ITO-coated glass substrate (coated area: 1.1 cm × 0.5 cm) in 0.1 M TBAP/CH_3CN with a cycle time of 14 s. (a) Current consumption and (b) absorbance change monitored at the given wavelength.

broad band having its maximum absorption wavelength at 1022 nm in the NIR region gradually increased in intensity. We attribute this spectral change in visible range to the formation of a stable monocation radical of the TPA center in TPPA moiety. Furthermore, the broad absorption in NIR region was the characteristic result due to IV-CT excitation associated with ET from active neutral nitrogen atom to the cation radical nitrogen center of TPPA moiety, which was consistent with the phenomenon classified by Robin and Day.[7] As the anodic potential increasing to 1.07 V, the absorption bands of the cation radical decreased gradually with a new broad band centered at around 815 nm. The disappearance of NIR absorption band can be attributable to the further oxidation of monocation radical species to the formation of dication in the TPPA segments. The observed UV–vis-NIR absorption changes in the **PAAI-2M** film at various potentials are fully reversible and are associated with strong color changes. The other PAAIs showed similar spectral change to that of **PAAI-2M** (as shown in Supporting Information Fig. S7). From the inset shown in Figure 3(a), the **PAAI-2M** film switches from transparent and pale yellow neutral form to highly absorbing semioxidized green form and fully oxidized blue form. The film colorations are distributed homogeneously across the polymer film and survive for more than hundreds of redox cycles. The polymer **PAAI-2M** shows high contrast both in the visible and NIR regions with an extremely high-optical transmittance change ($\Delta\%T$) of 63% at 422 nm and 60% at 1022 nm for green coloring at the first-oxidation stage, and 84% at 815 nm for blue coloring at the second-oxidation stage, respectively. Moreover, coloration changes were also observed in these PAAIs upon reduction. As shown in Figure 3(b), the **PAAI** films changed from yellow neutral form to a red reduced form, which also exhibited good contrast in the visible region with a high-optical transmittance change ($\Delta\%T$) of 58% at 481 nm for red coloring at the reduction stage. Thus, these **PAAI**s demonstrated a good combination of redox active TPPA and bis(trimellitimide)s units for the preparation of red, green, and blue (RGB) electrochromic materials.

Electrochromic Switching Studies

The stability, response time, and color efficiency are the key parameters for an electroactive polymer film to be amenable for usage in optical and electrochromic devices, thus the electrochromic switching studies were further measured. For electrochromic switching studies, polymer films were cast on ITO-coated glass slides in the same manner as described earlier, and chronoamperometric and absorbance measurements

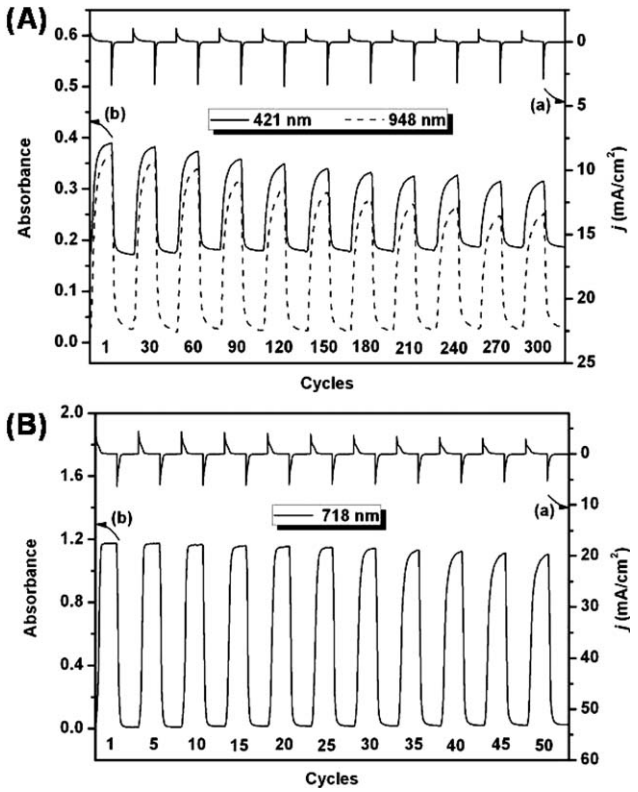

FIGURE 7 Electrochromic switching between (A) 0 and 0.85 V and (B) 0 and 1.35 V (vs. Ag/AgCl) of **PAAI-2M′** thin film (~270 nm in thickness) on the ITO-coated glass substrate (coated area: 1.1 cm × 0.5 cm) in 0.1 M TBAP/CH_3CN with a cycle time of 20 s. (a) Current consumption and (b) absorbance change monitored at the given wavelength.

TABLE 3 Optical and Electrochemical Data Collected for Coloration Efficiency Measurements of **PAAI-2M** and **PAAI-2M′**

			Q (mC/cm^2)[c]		η (cm^2/C)[d]		Decay (%)[e]	
Cycling Times[a]	**PAAI-2M** δOD_{422}[b]	**PAAI-2M′** δOD_{421}[b]	**PAAI-2M**	**PAAI-2M′**	**PAAI-2M**	**PAAI-2M′**	**PAAI-2M**	**PAAI-2M′**
1	0.573	0.390	3.223	1.565	178	249	0	0
30	0.570	0.382	3.223	1.563	177	244	0.56	2.01
60	0.570	0.372	3.223	1.559	177	239	0.56	4.02
90	0.570	0.359	3.223	1.541	177	233	0.56	6.43
120	0.565	0.348	3.221	1.537	175	226	1.69	9.24
150	0.564	0.338	3.221	1.532	175	221	1.69	11.24
180	0.560	0.333	3.220	1.526	174	218	2.25	12.45
210	0.560	0.325	3.219	1.521	173	214	2.81	14.06
240	0.559	0.324	3.219	1.511	173	214	2.81	14.06
270	0.553	0.314	3.217	1.505	172	209	3.37	16.06
300	0.547	0.313	3.216	1.504	170	208	4.49	16.47

[a] Switching between 0 and 0.74 for **PAAI-2M**, 0 and 0.85 for **PAAI-2M′**, respectively (V vs. Ag/AgCl).
[b] Optical density change at the given wavelength.
[c] Ejected charge, determined from the *in situ* experiments.
[d] Coloration efficiency is derived from the equation $\eta = \delta OD/Q$.
[e] Decay of coloration efficiency after cyclic scans.

were performed. Although the films were switched, the absorbance at the given wavelength was monitored as a function of time with UV–vis-NIR spectroscopy. Switching data for the representative cast film of polymer **PAAI-2M** (with 4,4′-dimethoxy-substituted) and **PAAI-2M′** (without 4,4′-dimethoxy-substituted) were shown in Figures 5–7 for comparison. The switching time was calculated at 90% of the full switch because it is difficult to perceive any further color change with naked eye beyond this point. As depicted in Figure 5(A), **PAAI-2M** film revealed switching time of 2.91 s at 0.76 V for coloring process at 422 nm and 1.32 s for bleaching. When the potential was set at 1.07 V, **PAAI-2M** film required 3.23 s for coloration at 815 nm and 2.05 s for bleaching [Fig. 5(B)]. The PAAIs switched rapidly between the highly transmissive neutral state and the colored oxidized state. As shown in Figures 6 and 7, the electrochromic stability of the polymer **PAAI-2M** and **PAAI-2M′** films were determined by measuring the optical change as a function of the number of switching cycles. The electrochromic CE ($\eta = \delta OD/Q$) and injected charge (electroactivity) after various switching steps were monitored and summarized in Tables 3 and 4. The electrochromic film of **PAAI-2M** was found to

TABLE 4 Optical and Electrochemical Data Collected for Coloration Efficiency Measurements of **PAAI-2M** and **PAAI-2M′**

			Q (mC/cm^2)[c]		η (cm^2/C)[d]		Decay (%)[e]	
Cycling Times[a]	**PAAI-2M** δOD_{815}[b]	**PAAI-2M′** δOD_{718}[b]	**PAAI-2M**	**PAAI-2M′**	**PAAI-2M**	**PAAI-2M′**	**PAAI-2M**	**PAAI-2M′**
1	1.311	1.173	5.410	5.316	242	221	0	0
5	1.311	1.173	5.410	5.315	242	221	0	0
10	1.311	1.165	5.410	5.315	242	219	0	0.95
15	1.311	1.157	5.410	5.313	242	218	0	1.36
20	1.311	1.149	5.410	5.313	242	216	0	2.26
25	1.311	1.146	5.410	5.313	242	216	0	2.26
30	1.310	1.141	5.409	5.313	242	215	0	2.71
35	1.304	1.125	5.409	5.311	241	212	0.41	4.07
40	1.297	1.124	5.408	5.311	240	212	0.83	4.07
45	1.285	1.108	5.407	5.311	238	209	1.65	5.43
50	1.279	1.100	5.407	5.311	237	207	2.07	6.33

[a] Switching between 0 and 1.16 for **PAAI-2M**, 0 and 1.35 for **PAAI-2M′**, respectively (V vs. Ag/AgCl).
[b] Optical density change at the given wavelength.
[c] Ejected charge, determined from the *in situ* experiments.
[d] Coloration efficiency is derived from the equation $\eta = \delta OD/Q$.
[e] Decay of coloration efficiency after cyclic scans.

show good CE up to 178 cm^2/C at 422 nm (185 cm^2/C at 1022 nm), and to retain more than 99% of their electroactivity after switching 300 times between 0 and 0.74 V [Fig. 6(A)]. As the applied switching potential increased to 1.16 V, a higher CE (242 cm^2/C at 815 nm) could be obtained and showed only 0.1% decay of its electroactivity after 50 cycles [Fig. 6(B)]. On the contrary, the corresponding **PAAI-2M′** without the para-methoxy substituted on TPPA units gradually lost δOD change after several cyclic switches (Fig. 7). The result also consists with the improvement of **PAAI-2M** in electrochemical studies by the introduction of para-substituted methoxy group on the TPPA unit.

CONCLUSIONS

A series of novel NIR electroactive TPPA-based PAAIs were readily prepared from the $(OMe)_2$TPPA-based diamine monomer with various aromatic diimide–diacids via the phosphorylation polyamidation reaction. Introduction of electron-donating para-methoxy substituted on TPPA unites not only stabilizes its cationic radicals and dications but also leads to good solubility and uniform amorphous films using solution-casting techniques. In addition to high T_g, good thermal stability, notable low-switching times, high CE, and excellent electroactive reversibility, the polymers also revealed interesting electrochromic characteristics with color change from pale yellow neutral state to green/blue oxidized states and red reduced state. The result provides the strategies for the design of functional polymers with RGB electrochromism. Thus, these characteristics suggest that these novel $(OMe)_2$TPPA-based PAAIs have great potential for multicolored electrochromic applications in both visible and NIR region.

We are grateful to the National Science Council of the Republic of China for financial support of this work.

REFERENCES AND NOTES

1 Monk, P. M. S.; Mortimer, R. J.; Rosseinsky, D. R. Electrochromism and Electrochromic Devices; Cambridge University Press: Cambridge, UK, 2007.

2 (a) Bach, U.; Corr, D.; Lupo, D.; Pichot, F.; Ryan, M. Adv Mater 2002, 14, 845–848; (b) Dyer, A. L.; Grenier, C. R. G.; Reynolds, J. R. Adv Funct Mater 2007, 17, 1480–1486; (c) Ma, C.; Taya, M.; Xu, C. Polym Eng Sci 2008, 48, 2224–2228; (d) Beaupre, S.; Breton, A. C.; Dumas, J.; Leclerc, M. Chem Mater 2009, 21, 1504–1513.

3 (a) Bange, K.; Gambke, T. Adv Mater 1990, 2, 10–16; (b) Mortimer, R. J. Chem Soc Rev 1997, 26, 147–156; (c) Rosseinsky, D. R.; Mortimer, R. J. Adv Mater 2001, 13, 783–793; (d) Somani, P. R.; Radhakrishnan, S. Mater Chem Phys 2003, 77, 117–133; (e) Lee, S. H.; Deshpande, R.; Parilla, P. A.; Jones, K. M.; To, B.; Mahan, H.; Dillon, A. C. Adv Mater 2006, 18, 763–766; (f) Zhang, T.; Liu, S.; Kurth, D. G.; Faul, C. F. J. Adv Funct Mater 2009, 19, 642–652; (g) Maier, A.; Rabindranath, A. R.; Tieke, B. Adv Mater 2009, 21, 959–963; (h) Li, M.; Sheynin, Y.; Patra, A.; Bendikov, M. Chem Mater 2009, 21, 2482–2488.

4 (a) Rose, T. L.; D'Antonio, S.; Jillson, M. H.; Kon, A. B.; Suresh, R.; Wang, F. Synth Met 1997, 85, 1439–1440; (b) Franke, E. B.; Trimble, C. L.; Hale, J. S.; Schubert, M.; Woollam, J. A. J Appl Phys 2000, 88, 5777–5784; (c) Topart, P.; Hourquebie, P. Thin Solid Films 1999, 352, 243–248.

5 (a) Vickers, S. J.; Ward, M. D. Electrochem Commun 2005, 7, 389–393; (b) Schwab, P. F. H.; Diegoli, S.; Biancardo, M.; Bignozzi, C. A. Inorg Chem 2003, 42, 6613–6615; (c) Wang, S.; Todd, E. K.; Birau, M.; Zhang, J.; Wan, X.; Wang, Z. Y. Chem Mater 2005, 17, 6388–6394; (d) Qiao, W.; Zheng, J.; Wang, Y.; Zheng, Y.; Song, N.; Wan, X.; Wang, Z. Y. Org Lett 2008, 10, 641–644; (e) Qi, Y.; Wang, Z. Y. Macromolecules 2003, 36, 3146–3151.

6 (a) Creutz, C.; Taube, H. J Am Chem Soc 1973, 95, 1086–1094; (b) Lambert, C.; Noll, G. J Am Chem Soc 1999, 121, 8434–8442.

7 Robin, M.; Day, P. Adv Inorg Radiochem 1967, 10, 247–422.

8 Szeghalmi, A. V.; Erdmann, M.; Engel, V.; Schmitt, M.; Amthor, S.; Kriegisch, V.; Noll, G.; Stahl, R.; Lambert, C.; Leusser, D.; Stalke, D.; Zabel, M.; Popp, J. J Am Chem Soc 2004, 126, 7834–7845.

9 (a) Thelakkat, M. Macromol Mater Eng 2002, 287, 442–461; (b) Shirota, Y. J Mater Chem 2005, 15, 75–93; (c) Shirota, Y.; Kageyama, H. Chem Rev 2007, 107, 953–1010; (d) Kuorosawa, T.; Chueh, C. C.; Liu, C. L.; Higashihara, T.; Ueda, M.; Chen, W. C. Macromolecules 2010, 43, 1236–1244.

10 (a) Oishi, Y.; Ishida, M.; Kakimoto, M. A.; Imai, Y.; Kurosaki, T. J Polym Sci Part A: Polym Chem 1992, 30, 1027–1035; (b) Liou, G. S.; Hsiao, S. H.; Ishida, M.; Kakimoto, M. A.; Imai, Y. J Polym Sci Part A: Polym Chem 2002, 40, 3815–3822; (c) Leung, M. K.; Chou, M. Y.; Su, Y. O.; Chiang, C. L.; Chen, H. L.; Yang, C. F.; Yang, C. C.; Lin, C. C.; Chen, H. T. Org Lett 2003, 5, 839–842; (d) Chou, M. Y.; Leung, M. K.; Su, Y. O.; Chiang, C. L.; Lin, C. C.; Liu, J. H.; Kuo, C. K.; Mou, C. Y. Chem Mater 2004, 16, 654–661; (e) Otero, L.; Sereno, L.; Fungo, F.; Liao, Y. L.; Lin, C. Y.; Wong, K. T. Chem Mater 2006, 18, 3495–3502.

11 (a) Cheng, S. H.; Hsiao, S. H.; Su, T. X.; Liou, G. S. Macromolecules 2005, 38, 307–316; (b) Su, T. X.; Hsiao, S. H.; Liou, G. S. J Polym Sci Part A: Polym Chem 2005, 43, 2085–2098.

12 (a) Liou, G. S.; Hsiao, S. H.; Su, T. X. J Mater Chem 2005, 15, 1812–1820; (b) Liou, G. S.; Yang, Y. L.; Su, Y. O. J Polym Sci Part A: Polym Chem 2006, 44, 2587–2603; (c) Liou, G. S.; Hsiao, S. H.; Chen, H. W. J Mater Chem 2006, 16, 1831–1842; (d) Liou, G. S.; Hsiao, S. H.; Huang, N. K.; Yang, Y. L. Macromolecules 2006, 39, 5337–5346; (e) Liou, G. S.; Chen, H. W.; Yen, H. J. J Polym Sci Part A: Polym Chem 2006, 44, 4108–4121; (f) Liou, G. S.; Chen, H. W.; Yen, H. J. Macromol Chem Phys 2006, 207, 1589–1598; (g) Liou, G. S.; Chang, C. W.; Huang, H. M.; Hsiao, S. H. J Polym Sci Part A: Polym Chem 2007, 45, 2004–2014; (h) Liou, G. S.; Yen, H. J.; Chiang, M. C. J Polym Sci Part A: Polym Chem 2009, 47, 5378–5385.

13 (a) Mazur, S.; Lugg, P. S.; Yarnilzky, C. J Electrochem Soc 1987, 134, 346–353; (b) Viehbeck, A.; Goldberg, M. J.; Kovac, C. A. J Electrochem Soc 1990, 137, 1460–1466; (c) Krause, L. J.; Lugg, P. S.; Speckhard, T. A. J Electrochem Soc 1989, 136, 1379–1385.

14 (a) Chang, C. W.; Liou, G. S.; Hsiao, S. H. J Mater Chem 2007, 17, 1007–1015; (b) Liou, G. S.; Chang, C. W. Macromolecules 2008, 41, 1667–1674; (c) Hsiao, S. H.; Liou, G. S.; Kung, Y. C.; Yen, H. J.

Macromolecules 2008, 41, 2800–2808; (d) Chang, C. W.; Chung, C. H.; Liou, G. S. Macromolecules 2008, 41, 8441–8451; (e) Chang, C. W.; Yen, H. J.; Huang, K. Y.; Yeh, J. M.; Liou, G. S. J Polym Sci Part A: Polym Chem 2008, 46, 7937–7949; (f) Yen, H. J.; Liou, G. S. Chem Mater 2009, 21, 4062–4070.

15 Yang, C. P.; Liou, G. S.; Yang, C. C.; Tseng, N. W. Polym Bull 1999, 42, 1–8.

16 Yang, C. P.; Liou, G. S.; Yang, C. C.; Chen, S. H. Polym Bull 1999, 43, 21–28.

17 Yang, C. P.; Liou, G. S.; Chang, S. Y.; Chen, S. H. J Appl Polym Sci 1999, 73, 271–278.

18 Yamazaki, N.; Matsumoto, M.; Higashi, F. J Polym Sci Polym Chem Ed 1975, 13, 1373–1380.

19 Cheng, S. H.; Hsiao, S. H.; Su, T. H.; Liou, G. S. Polymer 2005, 46, 5939–5948.

20 Wang, P.; Chai, C.; Yang, Q.; Wang, F.; Shen, Z.; Guo, H.; Chen, X.; Fan, X.; Zou, D.; Zhou, Q. J Polym Sci Part A: Polym Chem 2008, 46, 5452–5460; (b) Karastatiris, P.; Mikroyannidis, J. A.; Spiliopoulos, I. K. J Polym Sci Part A: Polym Chem 2008, 46, 2367–2378.

21 Liaw, D. J.; Chang, F. C.; Leung, M. K.; Chou, M. Y.; Muellen, K. Macromolecules 2005, 38, 4024–4029.